Journal of Low Temperature Physics, Vol. 129, Nos. 1/2, October 2002 (© 2002)

Distribution of ^{3}He–^{4}He Mixtures in a Bi-Porous System

G. Lawes,[1, (1)] E. Nazaretski,[1] P. N. Brusov,[1] N. Mulders,[2] and J. M. Parpia[1]

[1] *LASSP, Cornell University, Ithaca, New York 14853*
E-mail: glawes@lanl.gov
[2] *Department of Physics and Astronomy, University of Delaware, Newark, Delaware 19716*

(Received April 21, 2002; revised June 3, 2002)

We have investigated the distribution of ^{3}He–^{4}He mixtures in a system comprised of two porous materials: aerogel and silver sinter. The particle number density, and thus the ^{3}He–^{4}He concentration, was measured directly in the aerogel sample. We discuss both the observed history dependence for the low temperature equilibrium ^{4}He fraction in aerogel and the temperature evolution of the ^{4}He fraction.

Bulk ^{3}He–^{4}He mixtures exhibit a remarkable low temperature phase diagram.[1] The ^{4}He superfluid transition temperature decreases with an increasing ^{3}He fraction in the mixture, until it meets the phase separation curve at the tricritical point. Below 872 mK, the mixture undergoes phase separation into a ^{3}He-rich component and a superfluid ^{4}He-rich component. At zero temperature and pressure the ^{3}He rich phase excludes all ^{4}He impurities but a finite fraction of ^{3}He ($\approx 6.4\%$ at saturated vapor pressure) remains dissolved in the ^{4}He rich phase. Confining a ^{3}He–^{4}He mixture to a porous silica aerogel has been shown to alter this phase diagram.[2] In the presence of an aerogel impurity, the ^{4}He superfluid transition boundary and phase separation curve become detached, producing a range of ^{3}He fractions for which the mixture does not undergo true phase separation, but does exhibit a superfluid transition.

The observation of this modification in the ^{3}He–^{4}He phase diagram in aerogel led to intense theoretical[3–6] and experimental investigations into the problem of understanding low temperature ^{3}He–^{4}He mixtures in porous media. A quantitatively similar alteration of the ^{3}He–^{4}He phase diagram has been observed in a range of different aerogel samples,[7] in mixtures

[1] Current Address: Los Alamos National Laboratory, Los Alamos, New Mexico 87545.

0022-2291/02/1000-0049/0 © 2002 Plenum Publishing Corporation

confined to porous gold[8] and vycor glass[9] using a variety of measuring techniques.[10]

The cell used in our investigations was designed to probe the low frequency acoustical spectrum in ^{3}He–^{4}He mixtures in aerogel at ultra-low temperatures.[11] In order to cool the mixture below the ^{3}He superfluid transition temperature, the liquid was placed in contact with a silver sinter with a large surface area. This sinter provided a second volume of porous material in which the ^{3}He–^{4}He mixture could be distributed. By measuring the ^{4}He fraction in the aerogel (using an aerogel-filled concentric plate capacitor) as we varied the temperature of the sample, we were able to investigate the dynamics of ^{3}He–^{4}He mixtures in this bi-porous system. In contrast, all earlier investigations of ^{3}He–^{4}He mixtures in porous materials minimized the bulk volume in the experimental cavity, ensuring that the ^{4}He fraction of the mixture in the experimental cell was identical to the ^{4}He fraction added at room temperature. However, the experiments were restricted to the temperature regime above 100 mK.

1. EXPERIMENTAL DETAILS

Aerogel consists of a dilute network of silica stands. The particular aerogel used in our experiments was a base-catalyzed 98% porosity sample. Aerogels do not have a homogeneous distribution of silica, but exhibit density correlations.[12] For a typical 98% porosity sample, small angle X-ray scattering indicates that aerogel has a fractal microstructure on length scales from ≈ 4 nm to ≈ 100 nm. Since the silica strand structure of the aerogel does not lead to well-defined pores, we will describe the aerogel as having voids, or regions of low silica density, with characteristic lengths from 4 nm to 100 nm. This particular sample consists of a volume of 0.6 cm^3 with an estimated surface area of ≈ 15 m^2.

The distribution of ^{3}He–^{4}He mixtures confined to aerogel is determined by two main energy considerations. Firstly, the ^{4}He atoms have a smaller zero-point energy than the ^{3}He atoms, so the ^{4}He is preferentially attracted to the surface of the aerogel. Secondly, the mixture will be distributed so as to reduce the interfacial area between the ^{3}He and ^{4}He rich phases and minimize the interfacial (or surface) energy. The following picture has been proposed to describe the distribution of the ^{3}He and ^{4}He components of mixtures in aerogel when a comparable area of small-pore silver sinter was absent.[10]

With a mixture containing a ^{4}He fraction (x_4) of $\leqslant 4\%$, all of the ^{4}He atoms are localized in a disordered solid layer on the surface of the silica strands. Increasing x_4 produces a thin superfluid film over the strands, and this film thickens with increasing ^{4}He fraction. At an x_4 of $\approx 15\%$, once a

critical film thickness (corresponding to a coverage of approximately 4.5 nm) is achieved, adding ^{4}He to the system does not increase the thickness of the superfluid film. It should be pointed out that the width of the phase separation boundary is ≈ 1.5 nm, so there is no clear delineation between the ^{3}He rich and ^{4}He rich phases in the thin film regime. As x_4 is increased past $\approx 15\%$, the ^{4}He component of the mixture begins to form bridges between neighboring strands, and fills the regions of high silica density. This "capillary condensation" signals the onset of macroscopic regions of ^{4}He rich phase. An increase in ^{4}He leads to more of the smaller voids filling with the ^{4}He rich phase, leaving the ^{3}He rich phase to occupy the largest voids. At a ^{4}He fraction of around 93%, the sample is completely filled with the ^{4}He rich phase containing some fraction of dissolved ^{3}He. Our observations of the behavior of ^{3}He–^{4}He mixtures in an aerogel/silver sinter system agree very well with the predictions of this model.

In contrast to the fractal structure of silica aerogel, the sintered silver heat exchanger provides a simple porous material with a narrow pore size distribution. The sinter was made from 70 nm silver powder packed to 50% open volume and heated at 200°C for an hour. This leads to well defined, interconnected pores with an average diameter of 80 nm and a narrow distribution in pore sizes.[13] The open volume in this sinter is approximately 0.6 cm^3, with a surface area of 4.2 m^2. The surface area and open volumes are comparable to those measured by other investigators.[14–16] Besides the 0.6 cm^3 taken up the by aerogel and the 0.6 cm^3 filled by the silver sinter, there is approximately 0.8 cm^3 of bulk volume in this cell and fill lines. Note that orientation of the cell is the same as shown in Fig. 1, that is, the bottom of the aerogel sample is located approximately 3 cm above the silver sinter. This will be important when we discuss the energetics of this system.

A schematic diagram of the cell used in these investigations in shown in Fig. 1. The principal measurements in these experiments are done with a capacitor connected to the large resonator cavity and both the resonator and the capacitor were filled with 98% aerogel. The capacitor provided an *in situ* measurement of the ^{4}He number density in the aerogel sample which proved crucial to our investigation of the temperature dependence of x_4 (the ^{4}He fraction) in aerogel. The sound transducers were used to monitor the distribution of ^{4}He in the aerogel via changes in the "tortuosity" as manifested by changes of the resonant frequency of the sound modes.[17] Similar changes in the tortuosity were mapped in a torsion pendulum experiment.[18] The cell was cooled by a dilution refrigerator, and the temperature in this regime ($\geqslant 20$ mK) was measured using a calibrated 1 kΩ Dale resistor.

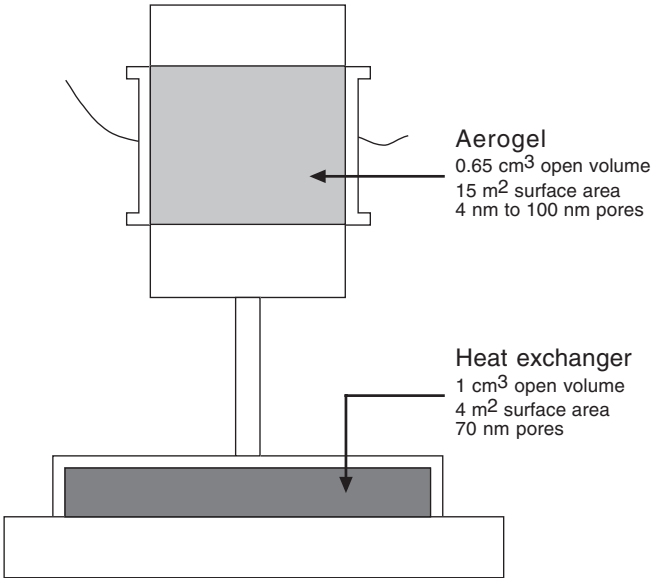

Fig. 1. Schematic diagram of the cell used for investigating the distribution of ^{3}He–^{4}He mixtures in aerogel and silver sinter.

2. CAPACITOR AND METHODOLOGY

The capacitor used to determine the ^{4}He fraction in the aerogel sample consists of two concentric stainless steel cylinders, filled with a 98% aerogel. Because the atomic polarizability of ^{3}He and ^{4}He are identical, the change in capacitance upon filling the cell depends solely on the total number density in the aerogel. We calibrated the device by measuring the empty cell capacitance, together with the capacitance at several different pressures (particle densities) with both pure ^{3}He and pure ^{4}He. The calibration was found to be:

$$\Delta C = 6.1331 \text{ pF } \rho \tag{1}$$

with ρ the particle density in mol/cm^3. The empty cell capacitance at low temperature was 4.5114 pF. Using this calibration, we were able to determine x_4 by converting the change in capacitance into a particle number density. Then, using bulk ^{3}He and ^{4}He molar volumes, we compute the relative ^{3}He and ^{4}He fractions in the mixture within the aerogel. The error introduced by using bulk molar volumes for the ^{3}He and ^{4}He particle densities is small because the aerogel only occupies approximately 2% of the

total volume. This capacitor allowed us to determine the ^{4}He fraction in the aerogel to within 1%.

3. ADDITION OF ^{3}HE AND ^{4}HE TO THE EMPTY SYSTEM

Our first set of measurements involved an investigation of the deposition of ^{3}He–^{4}He mixtures into the bi-porous cell at low temperatures. This was motivated by the observation that ^{3}He–^{4}He mixtures in aerogel prepared at temperatures less than 100 mK exhibit different superfluid properties of the ^{4}He component when compared with samples prepared at temperatures above phase separation and then cooled to low temperatures.[18,19] Figure 2 shows the change in capacitance as ^{3}He (lower plot) and ^{4}He (upper plot) is added to the cell below 100 mK. The aerogel and sinter

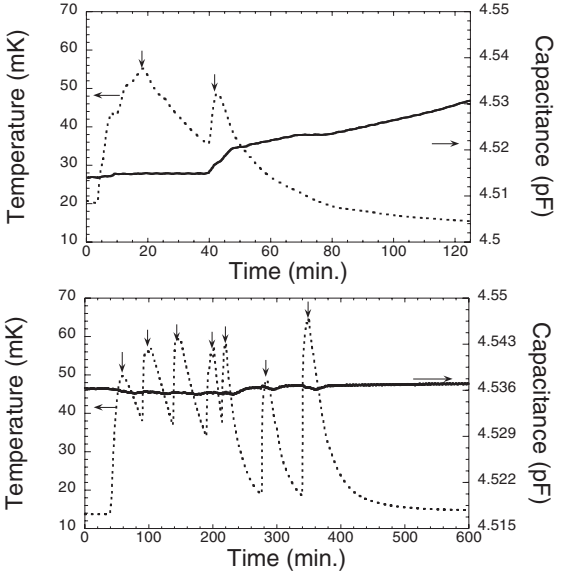

Fig. 2. The upper figure shows the capacitance change (solid lines) on the addition of pure ^{4}He into the system, which is preferentially deposited into the aerogel (as opposed to the sinter or the bulk). The vertical arrows mark the addition of ≈ 2 mmole pure ^{4}He to the system with a corresponding jump in temperature. The lower figure plots the change in capacitance as pure ^{3}He is added on to top of a small amount (4 mmole) of previously deposited ^{4}He. The vertical arrows indicate the addition of ≈ 2 mmole of ^{3}He. The capacitance is almost constant as the ^{3}He is added implying that the additional ^{3}He is preferentially attracted to the pores in the silver sinter.

are pre-plated with ≈ 2 mmole of ^{4}He (enough to deposit the localized solid layer) prior to the addition of more ^{4}He to the system. Each of the vertical arrows in the top portion of Fig. 2 marks the addition of 1–2 mmole of ^{4}He to the system, with a corresponding increase in temperature. Using the calibration from Eq. (1), we find that almost all the ^{4}He initially added to the cell at low temperatures is preferentially deposited in the aerogel, even after a solid layer of ^{4}He has been formed.[20] It should also be pointed out that the aerogel is located *above* the silver sinter, so it is gravitationally unfavorable for the ^{4}He to invade the aerogel rather than the sinter.

By contrast, ^{3}He added to the system first fills the silver sinter or bulk volume, as shown in the lower plot in Fig. 2. The capacitor measures practically no change in the helium number density in aerogel as ^{3}He is added after the deposition of a few mmoles ^{4}He in the aerogel.

We can understand this behavior by noting that the ^{3}He is deposited into the cell at temperatures well below the phase separation temperature. Because the solubility of ^{3}He in ^{4}He is small at these low temperatures, most of the ^{3}He added to the system will enter the ^{3}He rich phase. In order to minimize the interfacial energy between the ^{3}He rich and ^{4}He rich phases, as well as to minimize the free surface of the ^{3}He, it is preferable for the ^{3}He to be deposited in the pores of the silver sinter, rather than a configuration with the ^{3}He rich phase distributed over the ^{4}He covered aerogel strands. The pores of the silver sinter have a concave curvature and are connected by "necks" of smaller diameter. The ^{3}He phase can coat the surfaces in the sinter, minimizing both the free surface and the interfacial area as it capillary condenses in the necks and smaller pores first.

4. EJECTION OF ^{4}HE FROM AEROGEL

One further peculiarity involving the distribution of ^{3}He–^{4}He mixtures in a bi-porous aerogel/sinter system is the inability to create a ^{3}He–^{4}He mixture with an average ^{4}He fraction in the aerogel between approximately 3% and 10% (corresponding to roughly 2.5 to 7.5 mmole ^{4}He). This ^{4}He coverage should be enough to form a film. However, this distribution would have a large interfacial area between the pure ^{3}He and the dilute mixture. Given this large free energy cost, the ^{4}He film is unstable in the aerogel and is ejected into the silver sinter. The curvature in the sinter (primarily concavities) as compared to the mainly convex surfaces in the aerogel, would lead to a progressively larger interfacial energy in the aerogel as the film thickness increases, compared to the smaller interface area as the ^{4}He film thickens in the sinter. A similar effect has been

observed in previous investigations on ^{3}He–^{4}He mixtures in aerogel at ultra-low temperature.[18,19] With the progressive addition of ^{4}He to the mixture beyond the disordered solid layer on the aerogel, the ^{4}He atoms are mainly confined to the silver sinter. Only once there is a sufficient amount of ^{4}He in the system to begin capillary condensation in the smallest aerogel voids is it no longer energetically favourable for the ^{4}He to relocate to the pores of the silver sinter. Further addition of ^{4}He beyond this point leads to a rapid increase of x_4 in the aerogel.

Figure 3 gives evidence for a rapid ejection of ^{4}He from the aerogel as the sample is completely filled with ^{3}He. This trace was taken at low temperature as pure ^{3}He was added to the experimental volume that initially contained 3.6 mmol/cm^3 ^{4}He. By this point in the loading of the cell, the sinter had been completely filled with the ^{3}He rich phase. Each vertical arrow corresponds to 1.8 mmole of pure ^{3}He being added to the system. The drop in capacitance corresponding to the expulsion of approximately 3 mmol/cm^3, (circled in Fig. 3) is consistent with the amount of ^{4}He which would be required to relocate to the sinter to result to obtain the measured equilibrium ^{4}He concentration in the completely filled cell, $\approx 3\%$ for this sample. This expulsion of ^{4}He out of the aerogel is only possible because of the presence of the sinter, which provides an alternative reservoir for the ^{4}He rich phase.[21]

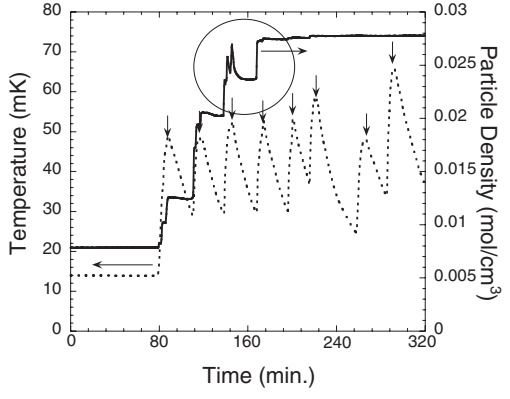

Fig. 3. Particle density as measured by the capacitor as the aerogel is filled with pure ^{3}He on top of 0.0036 mmole/cm^3 ^{4}He. Also shown is the temperature measured with a melting curve thermometer that exhibits heating spikes that correspond to the addition of increments of 1.8 mmole pure ^{3}He. The circled trace indicates the sudden exodus of ^{4}He into the pores of the silver sinter.

5. COLD DEPOSITED AND ANNEALED SAMPLES

The additional volume (and surface area) provided by the silver sinter also provides an explanation for the history dependence of the equilibrium ^{4}He concentration in the aerogel at low temperatures. For a given ^{3}He–^{4}He ratio at room temperature, samples prepared by depositing the mixture below 100 mK had larger ^{4}He fractions in the aerogel than samples prepared at 1 K and then cooled to 100 mK. We refer to the first case, where the mixture is "quench condensed" into cell at low temperatures, as *cold-deposited* samples, while the deposition from a homogenous mixture (not phase separated) starting from a high temperature (≈ 1 K) results in *annealed* samples. In practice, we first prepared the mixture in the cold-deposited state, then warmed the cell up to 1 K to produce the annealed state. As the cell was warmed and cooled, we observed striking changes in the ^{4}He fraction in the mixture in aerogel. We first consider, however, the variation of the low temperature ^{4}He fraction in the aerogel for cold deposited and annealed samples.

Figure 4 shows the ^{4}He fraction of the mixture in aerogel at 20 mK for a range of concentrations (x_4) of ^{4}He in the starting gas mixture at room temperature for both cold deposited and annealed mixtures. The ^{4}He concentrations corresponding to the solid ^{4}He that coats the strands and for complete filling with the ^{4}He rich phase are also shown. It is important to note that the ^{4}He fraction in the aerogel need not equal the ^{4}He fraction in the room temperature gas mixture because it is possible to have different values of x_4 in the aerogel and in the pores of the silver sinter. Even with a very small fraction ($\leqslant 2\%$) of ^{4}He in the starting room temperature mixture, the aerogel strands are coated by a solid layer of ^{4}He. For x_4 between 4% and 7% in the starting mix, a ^{4}He superfluid film is not formed on the aerogel, but instead the ^{4}He migrates preferentially to the sinter. Once a sufficient amount of ^{4}He ($\geqslant 7\%$) is added to the experimental volume, the aerogel strands are covered by a thin superfluid film whose thickness is unchanged as more ^{4}He is added to the system. Thus over a range of starting mixtures between 7% and 14%, x_4 in the aerogel remains fixed at $\approx 11\%$. Thus our observations of this bi-porous system were unable to sample x_4 between 4% and 11%. The solid layer of ^{4}He and the thin superfluid film show no change in their distribution as the system is warmed to 1K and cooled back down to 20 mK, as evidenced by the coincidence between the cold-deposited samples and their annealed equilibrium counterparts for small x_4. We conclude that these small x_4 depositions are equivalent irrespective of preparation method, and are close to their equilibrium distribution rather than forming some metastable interface.

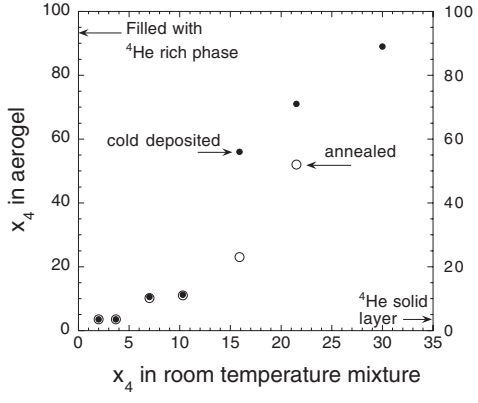

Fig. 4. ^{4}He fraction of the mixture in aerogel at 20 mK, for both cold-deposited (solid symbols) and annealed (open symbols) samples plotted against the ^{4}He fraction of the room temperature gas mixture. Also indicated by arrows are the ^{4}He fractions corresponding to the solid ^{4}He that covers the aerogel strands, and the ^{4}He fraction when the aerogel is completely filled with ^{4}He rich phase of the mixture.

The situation for values of x_4 greater than $\approx 15\%$, is very different. For these mixtures, the cold-deposited state has a significantly larger ^{4}He fraction than the annealed mixture. Even for relatively small values of x_4 in the room temperature mix, it is possible to prepare cold-deposited samples with a ^{4}He fraction of 71% in the mixture in aerogel. This high ^{4}He fraction in aerogel results from a non-equilibrium (as discussed below) distribution of the ^{4}He rich phase between the aerogel and silver sinter, with a much larger value of x_4 for the mixture confined to aerogel.

Unlike the mixtures in aerogel in the thin film state, the samples with larger values of x_4 show a dramatic shift in the equilibrium ^{4}He fraction on annealing the mixture at 1 K. The ^{4}He content of the mixture in the aerogel at 20 mK drops by between 18 to 30 mmole (or 30% to 50%) after the sample is annealed at 1 K. This suggests that the cold-deposited, high-x_4-in-aerogel state is metastable, and that a more uniform distribution of the ^{4}He component of the mixture between the aerogel and sinter is the equilibrium distribution.

We can estimate the potential energy stored in the metastable cold deposited state by computing the difference in gravitational potential difference between the high ^{4}He concentration cold deposited state and the low ^{4}He concentration annealed state. If we make the assumption that the ^{4}He leaving the aerogel is redistributed into the silver sinter, then changing

x_4 from $\approx 70\%$ to $\approx 20\%$ will reduce the gravitational potential energy by roughly 80 erg/cm^3, based on the difference in density between ^{3}He and ^{4}He at 10 bar and assuming a 3 cm displacement between the aerogel and sinter. Using the estimated value of the surface tension between the ^{3}He rich and ^{4}He rich phases in mixtures of 24 mdyne/cm,[22] this change in potential energy between the cold-deposited and annealed mixtures in aerogel corresponds to a interfacial area of $\approx 0.2\,\mathrm{m}^2$. This suggests a cold deposited mixture can only lower its free energy by redistribution of a fraction of the ^{3}He–^{4}He interfacial area.

6. HYSTERESIS AND TEMPERATURE DEPENDENCE OF x_4

We can also investigate the temperature dependence of x_4 in aerogel. Figure 5 plots the variation of x_4 in aerogel with temperature, for a cold-deposited sample (left panel) and an annealed sample (right panel), on both warming and cooling. Despite the fact that both samples begin with roughly the same ^{4}He content in the mixture confined to the aerogel, the dissimilarities in the temperature evolution of these two mixtures suggest that there is a significant variation in the spatial distribution of the ^{4}He rich phase in aerogel for cold-deposited versus annealed samples.

There are two main differences between the behavior of the cold-deposited versus annealed samples. Firstly, the cold-deposited sample shows evidence for hysteresis upon returning to the lowest temperature.

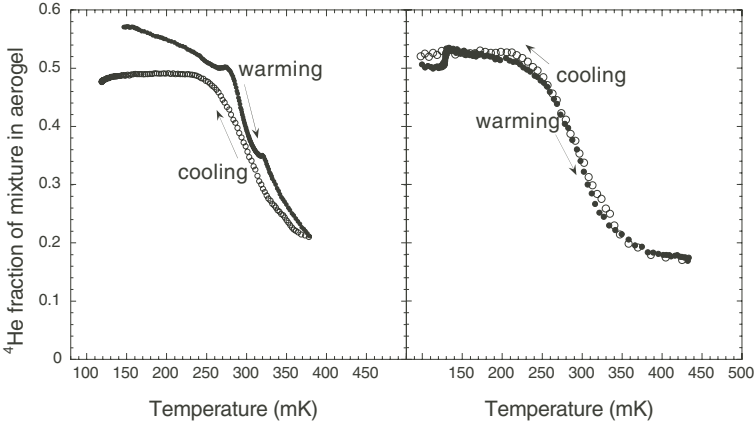

Fig. 5. Evolution of the ^{4}He fraction plotted versus temperature. The left panel shows the variations in a cold-deposited mixture upon warming (solid symbols) and subsequent cooling (open symbols). The right hand panel depicts a similar temperature variation for an annealed sample.

There is a substantial change in the ^{4}He fraction in aerogel before and after warming the sample to 400 mK. The annealed sample on the other hand shows no signs of such a variation of x_4. The small variations in x_4 with temperature in the annealed sample are likely due to variations in thermal gradients along the refrigerator column while the sample is warmed and cooled.

The second qualitative difference between these two plots is the presence of small peaks in the trace plotting the evolution of x_4 on warming the cold-deposited sample. These features are absent in all other traces in which the evolution of the ^{4}He fraction in aerogel is a monotonic function of temperature. We attribute the presence of these peaks to a thermally activated rearrangement of the ^{4}He rich phase domains inside the aerogel. The ^{4}He rich phase in the cold-deposited mixture is distributed in some non-equilibrium, but metastable, configuration. As the sample is warmed, the ^{4}He fraction in the cell drops because of migration of ^{4}He to other portions of the cell and because of the temperature dependence of the solubility of ^{3}He in ^{4}He (and *vice-versa*). However, there is also the possibility of an irreversible change in the distribution of the ^{4}He rich phase in aerogel, from a metastable to a thermodynamically stable configuration. The peaks in the evolution of x_4 could be evidence for the reorganization of the interface in the aerogel or between the components of the bi-porous system. Even though this sample was not warmed above the coexistence envelope (i.e., the sample was still phase separated below 400 mK) we note that on cooling the ^{4}He is apparently in a stable configuration so there are no sharp features corresponding to an irreversible redistribution of ^{4}He. The behavior on cooling (following the warming of the sample to near the coexistence curve) of the cold-deposited sample replicates the behavior of a nearly identical concentration annealed sample.

We also find evidence for hysteresis in the distribution of the ^{4}He rich phase in aerogel by examination of the acoustic spectrum of the sample. We measured the spectrum of ^{3}He–^{4}He mixtures in aerogel for samples prepared under different conditions, and found that the mode structure of the system displayed a strong history dependence. We plot in Fig. 6 the acoustic spectrum for a mixture in aerogel containing 89% ^{4}He at 20 mK, both for the cold deposited sample and for a sample annealed at 500 mK then cooled back to 20 mK. Note that distinct ^{3}He and ^{4}He rich phases of the mixture exist at a temperature of 500 mK so that the system does not undergo a complete remixing at this temperature(see Fig. 5). There are two peaks visible in each spectrum; resonance "A" is caused by second sound like mode of the superfluid ^{4}He component of the mixture, while resonance "B" arises from the Helmholtz mode, an oscillation of the normal component (primarily the ^{3}He-rich phase) in and out of the cell through the fill line. Similar features were observed for pure ^{3}He samples.[23, 11]

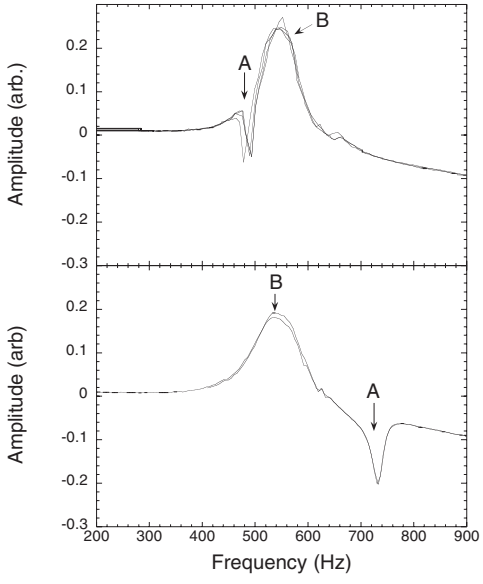

Fig. 6. Acoustic spectra for cold-deposited (upper) and annealed (lower) mixtures in aerogel containing 89% ^{4}He. These traces were taken at 20 mK. The feature labelled "A" is a resonance arising from the slow mode of superfluid ^{4}He, while the peak labelled "B" is attributed to a Helmholtz mode in the normal fluid.

The resonant frequency of the ^{4}He slow mode depends on both the ^{4}He fraction in the mixture in aerogel and on the distribution of the ^{4}He rich phase via the tortuosity.[17] Since the low temperature (20 mK) ^{4}He fraction in aerogel for this sample is unchanged on annealing to 500 mK, the shift in the slow mode resonant frequency must arise from a redistribution of the ^{4}He rich phase brought about by heating the sample. The higher frequency of the ^{4}He slow-mode on annealing is evidence of the lower tortuosity (or higher connectivity) of the ^{4}He film.

Our final experiment on the ^{4}He fraction in aerogel dependence on temperature involved a sample with a very high ^{4}He fraction. We investigated the temperature evolution of x_4 for an annealed mixture with an initial ^{4}He fraction of 89%. This sample showed a decrease in x_4 as the sample was warmed, consistent with the increased solubility of ^{3}He in ^{4}He at higher temperatures. The evolution of the ^{3}He fraction of the mixture in aerogel with temperature variation is plotted together with the phase diagram for ^{3}He–^{4}He mixtures in aerogel (taken from Ref. 2) in Fig. 7.

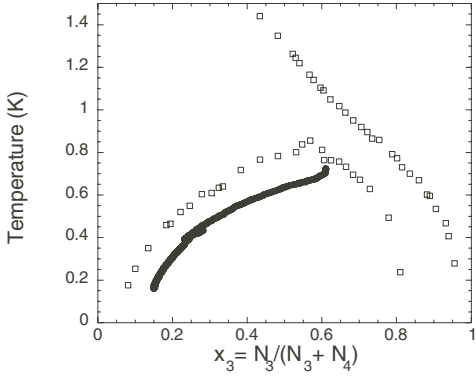

Fig. 7. Evolution of ^{3}He fraction of the mixtures in aerogel with temperature plotted for a sample containing 89% ^{4}He at 20 mK and 17.2 bar (solid symbols). Also shown on this figure is the ^{3}He–^{4}He phase diagram in aerogel (open squares).

The low temperature ^{3}He distribution in this mixture is expected to consist of isolated pockets of pure ^{3}He confined to the largest voids in the aerogel sample, together with the $\approx 8\%$ ^{3}He dissolved in the ^{4}He rich phase at this pressure.[24] A ^{4}He fraction of 89% leaves approximately 4% of the open volume in the aerogel filled with pure ^{3}He. This 4% pure ^{3}He is close to the offset between the phase separation curve for ^{3}He–^{4}He mixtures in aerogel and the low temperature equilibrium ^{3}He fraction shown in Fig. 7. As the mixture is warmed, the trace parallels the phase separation curve, at least for temperatures below 400 mK. The feature at 450 mK is the result of allowing the sample to cool briefly before resuming the heating. The distribution of the ^{4}He rich phase shows negligible hysteresis during this thermal loop, as expected in an annealed sample.

We can draw some conclusions about the distribution of the mixture inside the aerogel based on the proximity of the phase separation curve to the trace of temperature versus ^{3}He fraction for this sample. It must be the case that at low temperatures, additional ^{3}He is added to the mixture *only* through the increased solubility of ^{3}He in the ^{4}He rich phase at higher temperatures. That is, the boundaries of the regions of ^{3}He-rich mixture are largely unchanged as the sample is warmed, and there are no additional bubbles of ^{3}He-rich mixture formed. This is consistent with previously proposed models for the distribution of the ^{3}He and ^{4}He rich phases for helium mixtures in porous gold which suppose that as x_3 is reduced, the radius of curvature of the pure ^{3}He bubbles remain unchanged, but the fractional volume occupied by these bubbles is reduced.

7. CONCLUSIONS

An investigation on the distribution of ^{3}He–^{4}He mixtures in aerogel connected to a silver sinter leads to a fuller understanding of binary fluids in porous media. In particular, the silver sinter acts as a reservoir allowing the ^{4}He fraction of the mixture in the aerogel to evolve with temperature. This allows observations on the temperature dependence of the equilibrium ^{4}He concentration in aerogel, and well as enables the opportunity to study the metastable distributions formed when a ^{3}He–^{4}He mixture is quench condensed into the cell at low temperatures. Although the strong history dependence and complicated distribution of the ^{4}He rich phase in the aerogel make a detailed investigation of the dynamics of ^{3}He–^{4}He mixtures in aerogel and sinter intractable, our observations on the evolution of x_4 with temperature agree with the model proposed for understanding the distribution of ^{3}He–^{4}He mixtures in aerogel.[10] Specifically, we find that the onset of hysteretic behavior on warming and cooling the sample coincides with the onset of the development of macroscopic filled voids of ^{4}He rich phase in the aerogel. Also on the ^{4}He rich side of the phase diagram, the ^{3}He rich phase is confined in isolated bubbles which do not coalesce into larger ^{3}He filled regions until close to the phase separation temperature. We believe that further investigations of binary mixtures in a bi-porous system will reveal new behavior that will aid in understanding the spatial distribution of these mixtures confined to a single porous medium.

This research was supported by a grant from the National Science Foundation DMR-9970817.

REFERENCES

1. E. H. Graf, D. M. Lee, and J. D. Reppy, *Phys. Rev. Lett.* **19**, 417 (1967).
2. S. B. Kim, J. Ma, and M. H. W. Chan, *Phys. Rev. Lett.* **71**, 2268 (1993).
3. L. Pricaupenko and J. Treiner, *Phys. Rev. Lett.* **74**, 430 (1995).
4. A. Falicov and A. N. Berker, *Phys. Rev. Lett.* **74**, 426 (1995).
5. A. Maritan, M. Cieplak, M. Swift, F. Toigo, and J. R. Banavar, *Phys. Rev. Lett.* **69**, 221 (1992).
6. M. Boninsegni and D. M. Ceperley, *Phys. Rev. Lett.* **74**, 2288 (1995).
7. Jongsoo Yoon, N. Mulders, and M. H. W. Chan, *J. Low Temp. Phys.* **110**, 585 (1998).
8. D. J. Tulimieri, J. Yoon, and M. H. W. Chan, *Phys. Rev. Lett.* **82**, 121 (1999).
9. T. Hohenberger, R. Konig, and F. Pobell, *J. Low Temp. Phys.* **110**, 579 (1998).
10. N. Mulders and M. H. W. Chan, *Phys. Rev. Lett.* **75**, 3705 (1995).
11. G. Lawes, E. Nazaretski, P. Brusov, N. Mulders, and J. M. Parpia, submitted to *Phys. Rev. Lett.*, (2001).
12. J. V. Porto and J. M. Parpia, *Phys. Rev. B* **59**, 14853 (1998).
13. D. J. Cousins, S. N. Fisher, A. M. Guenault, G. R. Pickett, E. N. Smith, and R. P. Turner, *Phys. Rev. Lett.* **73**, 2583 (1994).
14. H. Franco, J. Bossy, and H. Godfrin, *Cryogenics* **24**, 477 (1984).
15. P. A. Busch, S. P. Cheston, and D. S. Greywall, *Cryogenics* **24**, 445 (1984).

16. T. Hall, S. M. Tholen, K. R. Lane, V. Kotsubo, and J. M. Parpia, *J. Low Temp. Phys.* **89**, 897 (1992).
17. A ^{4}He thin film on aerogel follows the contour of the aerogel surface. The geometric "tortuosity" of the path is a measure of the connectivity of the ^{4}He film. A greater number of connections between adjacent strands of aerogel results in a shorter effective length of the ^{4}He film. This decreases the "index of refraction" of the ^{4}He and increases the velocity as well as the resonant frequency of the ^{4}He film's sound mode.
18. A. Golov, J. V. Porto, and J. M. Parpia, *J. Low Temp. Phys.* **110**, 591 (1998).
19. A. Golov, J. V. Porto, and J. M. Parpia, *Phys. Rev. Lett.* **80**, 4486 (1998).
20. We emphasize that the resolution of the capacitor cannot give information on the distribution of the ^{4}He on the scale of a monolayer. Rather, we describe the distribution of thicker films, where the van der Waals forces that would otherwise distribute the films more or less equally over the silver and silica surfaces do not dominate. We note that in Fig. 2, after an initial delay in which no ^{4}He appears in the capacitor there is a gradual increase in the number density, and the change in capacitance corresponds to nearly 90% of the ^{4}He admitted to the cell.
21. It is our observation that for this concentration, the ^{4}He rich phase does not occupy the open volume of the cell, and is instead confined to the sinter. It is likely that there is nothing particularly special about silver sinter other than its large surface area and preponderance of concave voids as compared to the primarily convex surfaces that bound the voids in aerogel.
22. A. Sato, K. Ohishi, and M. Suzuki, *J. Low Temp. Phys.* **107**, 165 (1997).
23. A. Golov, D. A. Geller, N. Mulders, and J. M. Parpia, *Phys. Rev. Lett.* **82**, 3492 (1999).
24. G. E. Watson, J. D. Reppy, and R. C. Richardson, *Phys. Rev.* **188**, 384 (1969).